J|A|C|S COMMUNICATIONS

Published on Web 09/07/2010

The Stabilizing Effect of Silicate on Biogenic and Synthetic Amorphous Calcium Carbonate

Assaf Gal, Steve Weiner, and Lia Addadi*

Weizmann Institute of Science, Department of Structural Biology, Rehovot 76100, Israel

Received August 2, 2010; E-mail: lia.addadi@weizmann.ac.il

Abstract: Silicate ions increase the thermal stability of the unstable amorphous calcium carbonate (ACC). This effect was observed first by comparing ACC from two different species of cystoliths, small calcified bodies formed in the leaves of some plants. The temperature of crystallization to calcite in the silicate-rich cystoliths from *M. alba* is 100 °C higher than that of the silicate-poor cystoliths from *F. microcarpa*. The stabilizing effect is confirmed *in vitro* with synthetic samples differing in their silicate content. With increasing silicate concentration in ACC, the crystallization temperature to calcite also increases. A mechanism of geometric frustration is suggested, whereby the presence of the tetrahedral silicate ion in the flat carbonate lattice prevents organization into crystalline polymorphs.

A fundamental question relevant for both biogenic and synthetic minerals is the manner in which metastable phases are stabilized. Metastable minerals such as ferrihydrite, amorphous calcium phosphate, and amorphous calcium carbonate are commonly produced by organisms.[1] In some cases they are stabilized throughout the lifetime of the organism, whereas in other cases they serve as precursor phases that subsequently transform into crystalline minerals.[2] Many different organisms are now known to use disordered mineral phases as precursors to their crystalline mature product.[3]

Amorphous calcium carbonate (ACC) is a widely explored case, in which the thermodynamically unstable amorphous phase is stabilized.[3−7] Analyses of biogenic calcium carbonates have identified the presence of phosphate anions and magnesium cations, which were associated with ACC and poorly ordered calcite.[8−11] Both of these additives are known to stabilize ACC *in vitro*.[8,12] These ionic additives are thought to prevent crystal nucleation and growth by interfering with the formation of an ordered crystalline structure of calcium carbonate.[13]

Cystoliths are small calcified bodies that are present in plants from some families of angiosperms.[14] They develop as ingrowths of the inner cell wall within specialized epidermal cells of the leaves.[15] The bulk of the cystolith is composed of hydrated ACC containing roughly one molecule of water per carbonate ion.[16] Generally, the cystolith contains a stalk composed of a silicate phase that connects the ACC body to the outer cell wall surface.[14,17] The cystolith ACC is stabilized *in vivo* throughout the life of the leaf. After extraction from the leaf the cystoliths remain amorphous under dry conditions at ambient temperature.[18] The cystolith function in leaves is unclear, as is the evolutionary advantage of using ACC or its stabilization mechanism.

Heating ACC is one way to measure its stability.[19,20] When heated, ACC loses bound water, and when the temperature is high enough to overcome the kinetic energy barrier, ACC crystallizes to calcite, the thermodynamically stable polymorph. Here we demonstrate that cystoliths with a high concentration of silicate ions in the ACC phase are more stable than cystoliths devoid of silicate. We also show that silicate ions stabilize ACC *in vitro*.

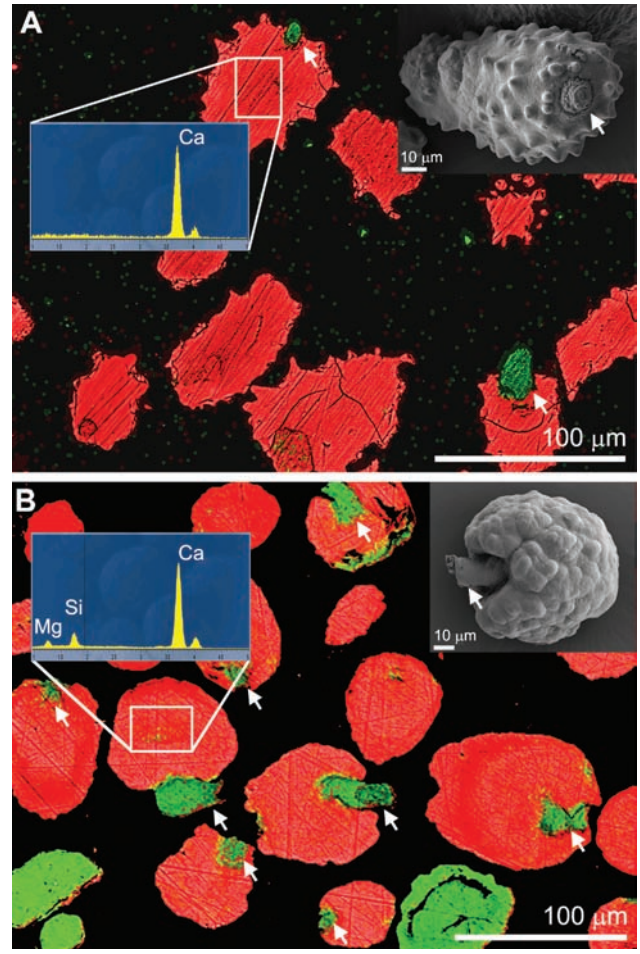

Figure 1. Elemental maps of cross sections through cystoliths from *F. microcarpa* (A) and *M. alba* (B), detected by EDS analysis. Red denotes calcium, and green, silicon. The spectrum in the inset is taken from the area specified on the map. The upper right insets are scanning electron microscope images of extracted cystoliths. Arrows indicate the silicate stalks of the cystoliths in the maps and insets.

Elemental mapping by energy dispersive X-ray spectroscopy (EDS) shows striking differences between the cross sections of cystoliths extracted from two different species of trees. The cystoliths from *Ficus microcarpa* (Moraceae) have small stalks, visible only in a few sections, whereas cystoliths from *Morus alba* (Moraceae) have much larger stalks, exposed in almost all sections (Figure 1). The EDS spectrum of the ACC phase of cystoliths from *F. microcarpa* contains no Si peak, whereas cystoliths from *M. alba* have a small Si peak (Figure 1). Accordingly, inductively

10.1021/ja106883c

Table 1. Major Element Composition (mol %)[a] in ACC Samples Analyzed by ICP-OES

Sample	%Ca	%Si	%Mg	%Na	%K	%P
F. microcarpa cystoliths	96.9 ± 0.1	0.06 ± 0.01	2.22 ± 0.01	0.333 ± 0.005	0.22 ± 0.01	0.009 ± 0.006
M. alba cystoliths	88.2 ± 0.4	0.96 ± 0.01	8.55 ± 0.05	0.057 ± 0.007	1.84 ± 0.04	0.063 ± 0.005
Synthetic ACC 0 mM Si	96.1 ± 0.2	0.04 ± 0.01	<0.01	3.80 ± 0.06	<0.01	<0.01
Synthetic ACC 3 mM Si	95.0 ± 0.1	1.06 ± 0.01	<0.01	3.92 ± 0.07	<0.01	<0.01
Synthetic ACC 9 mM Si	92.3 ± 0.2	3.19 ± 0.04	<0.01	4.45 ± 0.03	<0.01	<0.01
Synthetic ACC 15 mM Si	85.4 ± 0.4	7.22 ± 0.05	<0.01	7.39 ± 0.03	<0.01	<0.01

[a] The mol % refers to the sum total of Ca + Si + Mg + Na + K + P.

coupled plasma optic emission spectroscopy (ICP-OES) elemental analyses of the soluble ACC phase showed that the Si concentration in the *M. alba* cystoliths is 1 order of magnitude higher than the Si concentration in the *F. microcarpa* cystoliths (Table 1).

We monitored the thermal stability of the cystoliths by measuring their transition temperature to calcite, using Fourier transform infrared (FTIR) spectroscopy. The *F. microcarpa* cystolith spectrum at room temperature has the characteristics of ACC, namely a split $\nu 3$ peak at 1480 cm^{-1} and 1420 cm^{-1}, $\nu 1$ peak at 1075 cm^{-1}, $\nu 2$ peak at 865 cm^{-1}, and no detectable $\nu 4$ peak.[3] The ACC is still stable at 120 °C, although a slight broadening of the peaks is noted. At 160 °C some of the ACC crystallizes into calcite, identified by the appearance of the 875 and 713 cm^{-1} peaks. By 200 °C the spectrum is composed entirely of calcite, based on the presence of the single $\nu 3$ peak at 1425 cm^{-1}, the absence of the $\nu 1$ peak, a sharp $\nu 2$ peak at 875 cm^{-1}, and the $\nu 4$ peak at 713 cm^{-1} (Figure 2a). Cystoliths from *M. alba* showed a similar trend, but with two notable differences: strong silicate ion vibrations appear at 1080 and 470 cm^{-1} due to the presence of the relatively abundant silicate phase, and the transition to calcite is complete at around 300 °C, which is about 100 °C higher than the corresponding temperature of the *F. microcarpa* cystoliths (Figure 2b).

We hypothesized that the reason for the higher thermal stability of ACC from *M. alba* is related, in part, to the higher silicate ion content of the ACC phase. To test this hypothesis we synthesized ACC *in vitro*, using rapid precipitation from a supersaturated solution and adding increasing amounts of silicate ions to the reaction. We analyzed the ACC that precipitated from solutions containing no Si, 3 mM Si, 9 mM Si, and 15 mM Si. The actual Si concentrations in the precipitates were determined using ICP-OES (Table 1).

The IR spectra of the precipitates showed the carbonate peaks characteristic of ACC. A silicate peak was visible in the two samples containing the highest Si concentrations at 1050 cm^{-1} (Figure 3). The thermal stability of the synthetic ACC was then determined by heating the precipitates and monitoring changes in the IR spectrum. The calcium carbonate phase transition was determined using the same criteria as those for the biogenic samples. The homogeneity of the synthetic samples enabled better temperature resolution than that for the biogenic ones. For each synthetic sample a transition temperature range of 20 °C was determined. At the lower end of the temperature range the spectrum contains the typical $\nu 2$, $\nu 3$, and $\nu 4$ peaks of ACC, whereas at the higher end of the temperature range the spectrum contains the $\nu 2$, $\nu 3$, and $\nu 4$ peaks of calcite. In the midtemperature range the spectrum is a mixture of both phases.

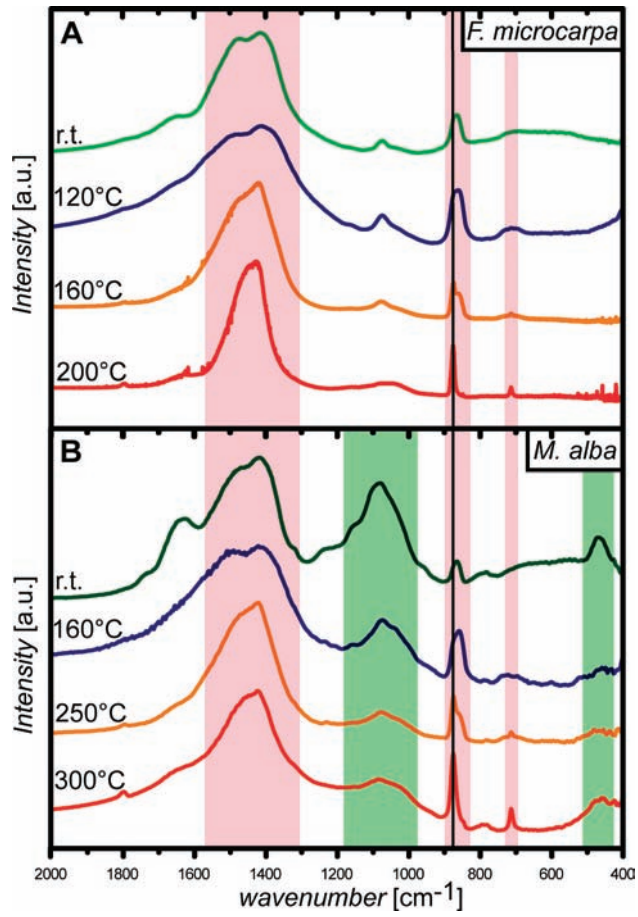

Figure 2. FTIR spectra monitoring the temperature-induced crystallization of cystoliths from *F. microcarpa* (A) and *M. alba* (B). For each species spectra were taken at different temperatures: at room temperature (green), at a higher temperature where the cystoliths are still amorphous (blue), at an intermediate temperature showing both ACC and calcite (orange), and at a temperature showing complete transformation to calcite (red). The line at 875 cm^{-1} is drawn to emphasize the $\nu 2$ peak shift. Red background: carbonate vibrations; green background: silicate vibrations.

The transition temperature of the synthetic ACC samples increases as the silicate concentration in the solution increases (Figure 3). The synthetic ACC without silicate is stable up to 250−270 °C. The synthetic ACC precipitated from the solution containing 3 mM Si is stable up to 260−280 °C, a small but significant difference, representing the onset of a stabilizing effect of the silicate anions. The synthetic ACC precipitated from the solution containing 9 mM Si shows elevated thermal stability and is stable up to 350−370 °C. The synthetic ACC precipitated from solutions containing 15 mM Si shows the highest thermal stability, with a crystallization temperature of 390−410 °C and a pronounced silicate peak at 1050 cm^{-1}. In the last two samples the position of the silicate peak in the FTIR spectrum above 350 °C is shifted to 950 cm^{-1}, suggesting a change in the silicate anion molecular environment.

We took advantage of the homogeneity of the synthetic samples to check ACC stability using different methods. Differential scanning calorimetry (DSC) traces show the exothermic peaks of the crystallization process. Such peaks are not visible in the biogenic samples due to differences within the biomineral causing broadening of the peaks to an undetectable size. The DSC results are consistent with the IR analyses and show elevated crystallization temperatures in the silicate-rich ACC (Figure 4). The exothermic peak indicative of the crystallization process appears at 282 °C in the silicate-free

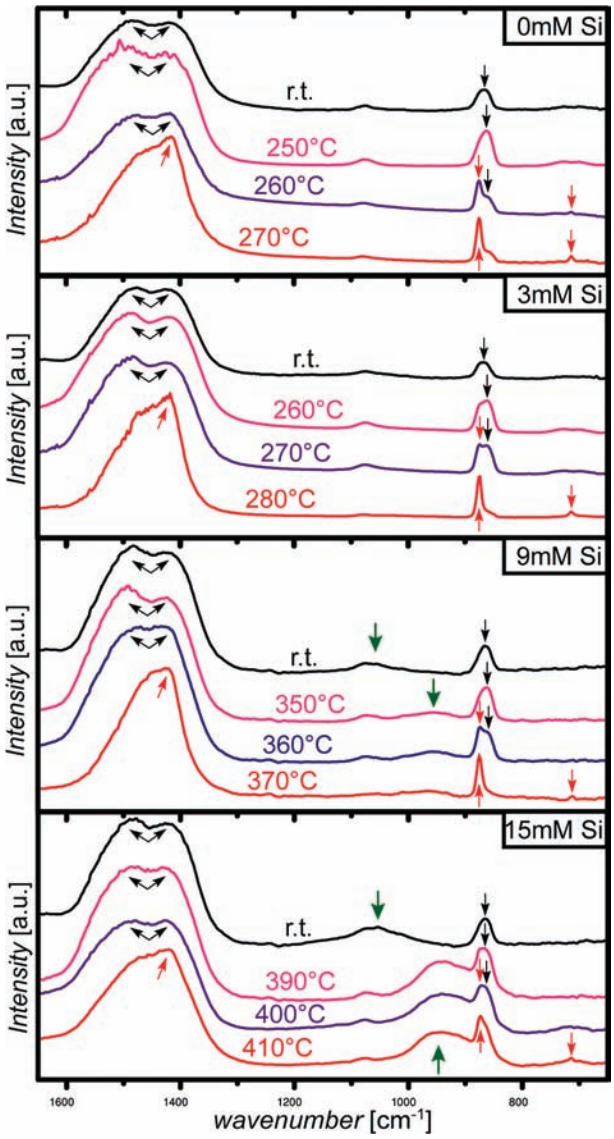

Figure 3. FTIR spectra of synthetic calcium carbonates precipitated in solutions containing 0, 3, 9, and 15 mM silicate, before and after their transformation from ACC to calcite. For each sample, spectra are shown: at room temperature (black), at the highest temperature where only ACC is observed (pink), at 10 °C higher than the former showing nascent calcite peaks (purple), and at the lowest temperature where full calcitic character was observed (red). Arrows indicate characteristic vibrations of each phase: black arrows = ACC, red arrows = calcite, and green arrows = silicate.

ACC, at 348 °C in the ACC that precipitated in the presence of 3 mM Si, and at 384 °C in the presence of 9 mM Si. The ACC that precipitated in the presence of 15 mM Si does not have a significant peak up to 390 °C, the operating limit of the DSC. The peak temperatures reflect both the thermodynamic and kinetic properties of the process. Being affected by the heating rate as well as by the thermal stability, they differ from the temperatures defined by the IR measurements.

The silicate induced stability of the synthetic ACC mirrored the trend observed in the cystoliths; i.e., a higher silicon content in the ACC correlates with higher thermal stability. Although the general trend is similar, the initial crystallization temperature and the influence of the silicon content are different for the synthetic ACC samples and for the cystoliths. In the cystoliths, the Si concentrations in the two species are 0.06% and 0.97% (Table 1), and the difference in their thermal stability is about 100 °C (Figure 2). In

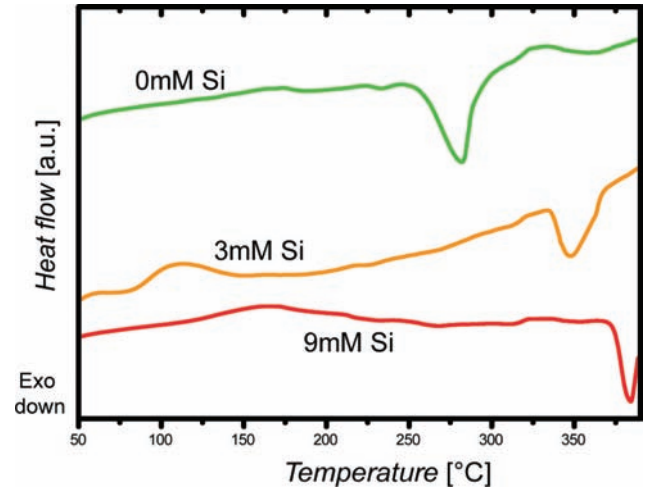

Figure 4. DSC traces of three synthetic ACC samples that precipitated from solutions containing different concentrations of sodium silicate. Heating rate: 5 °C min^{-1}.

the first two synthetic ACC samples, similar values of silicon content result in a minimal enhancement of the thermal stability by 10 °C (Figure 3). Moreover, the pure synthetic ACC is stable up to 250−270 °C, while the *F. microcarpa* cystoliths, which are almost silicate-free, start to crystallize around 160 °C.

These phenomena might reflect fundamental differences in the composition and/or precipitation conditions of the biogenic and synthetic ACC. Although the exact precipitation mechanism of cystoliths has not been investigated, other calcium carbonate biominerals are known to form in constrained environments, usually in subcellular vesicles, and at near physiological pH.[1] On the other hand our synthetic ACC samples were formed in a mixed solution at pH ≈ 11. The pH influence on the stability of ACC was tested and was shown to have a stabilizing role on the ACC.[20] Indeed, ACC that precipitates by mixing a calcium chloride solution with a sodium bicarbonate solution (at pH ≈ 8) is stable only up to 160−180 °C (Supporting Information). The different pH conditions might thus be the major factor stabilizing the silicate-poor synthetic ACC relative to the silicate-poor cystoliths.

An additional difference between the two cystolith species is their Mg contents. The four times higher Mg concentration of the *M. alba* cystoliths may contribute to their higher stability but it is unlikely to be solely responsible for the stability difference. A Mg content of 8%, similar to that for the *M. alba* cystoliths, was shown to induce only a slight delay in the crystallization of synthetic ACC in solution.[8] Other biogenic calcium carbonate samples having a similar Mg content happen to be crystalline or amorphous, implying that other factors are important for ACC stabilization in the presence of Mg.[3,11,21]

A possible mechanism for the stabilization of ACC by the silicate ions may be the destabilization of calcite by "geometric frustration" of the crystal lattice.[22] The calcite lattice, as all other crystalline calcium carbonates, incorporates the planar carbonate ions. The presence of the large tetrahedral silicate ions with four negative charges in the ACC may conceivably destabilize calcite both by preventing regular packing and by perturbing the charge equilibrium. This mechanism may be valid for both single silicate anions and for oligomers of polymerized silicate anions. The exact species of the silicate ions has to be determined for both biogenic and synthetic ACC.

The use of a tetrahedral ion to stabilize ACC is a known strategy in biomineralization: many biogenic ACC examples contain

relatively large amounts of phosphate. The phosphate ion also has a tetrahedral structure and has been suggested to stabilize ACC in the lobster carapace by a mechanism similar to what we suggest here for the silicate ion.[19] The cellular machinery of all organisms uses phosphates in various physiological reactions. Plants, unlike animals, have evolved various cellular mechanisms to transport and utilize silicate ions.[23] For example, silicate ions are the source for silica biomineral deposits in many plant tissues.[24] Cystoliths may be a case in which the ability of plants to utilize silicate led to the use of silicate as a stabilizing agent for ACC, corresponding to the role of phosphate in animal ACC.

The identification of silicate as a novel ACC stabilizing additive, revealed by its presence in cystoliths, may have implications in several fields of materials science, where it can be adopted to achieve desired materials properties. The concept of using ionic additives with different molecular geometry and charge to stabilize amorphous phases can be also expanded to other areas of bioinspired research where amorphous phases are desirable.

Acknowledgment. We thank Dr. Michael Bendikov for providing the DSC calorimeter and Dr. Eugenia Klein for help with the EDS measurements. This work was supported by Department of Energy Award DE-FG02-07ER15899. L.A. is the incumbent of the Dorothy and Patrick Gorman Professorial Chair of Biological Ultrastructure, and S.W. of the Dr. Trude Burchardt Professorial Chair of Structural Biology.

Supporting Information Available: Details of experimental procedures and additional results. This material is available free of charge via Internet at http://pubs.acs.org.

References

(1) Lowenstam, H. A.; Weiner, S. *On Biomineralization*; Oxford University Press: New York, 1989.
(2) Weiner, S.; Sagi, I.; Addadi, L. *Science* **2005**, *309* (5737), 1027–1028. Politi, Y.; Metzler, R. A.; Abrecht, M.; Gilbert, B.; Wilt, F.; Sagi, I.; Addadi, L.; Weiner, S.; Gilbert, P. U. P. A. *Proc. Natl. Acad. Sci. U.S.A.* **2008**, *105*, 17362–17366.
(3) Addadi, L.; Raz, S.; Weiner, S. *Adv. Mater.* **2003**, *15* (12), 959–970.
(4) Gebauer, D.; Volkel, A.; Colfen, H. *Science* **2008**, *322* (5909), 1819–1822.
(5) Pouget, E. M.; Bomans, P. H. H.; Goos, J. A. C. M.; Frederik, P. M.; de With, G.; Sommerdijk, N. A. J. M. *Science* **2009**, *323* (5920), 1455–1458.
(6) Wang, D. B.; Wallace, A. F.; De Yoreo, J. J.; Dove, P. M. *Proc. Natl. Acad. Sci. U.S.A.* **2009**, *106* (51), 21511–21516.
(7) Aizenberg, J.; Muller, D. A.; Grazul, J. L.; Hamann, D. R. *Science* **2003**, *299* (5610), 1205–1208.
(8) Loste, E.; Wilson, R. M.; Seshadri, R.; Meldrum, F. C. *J. Cryst. Growth* **2003**, *254* (1−2), 206–218.
(9) Aizenberg, J.; Lambert, G.; Weiner, S.; Addadi, L. *J. Am. Chem. Soc.* **2002**, *124* (1), 32–39.
(10) Becker, A.; Ziegler, A.; Epple, M. *Dalton Trans.* **2005**, (10), 1814–1820.
(11) Raz, S.; Weiner, S.; Addadi, L. *Adv. Mater.* **2000**, *12* (1), 38.
(12) Clarkson, J. R.; Price, T. J.; Adams, C. J. *J. Chem. Soc., Faraday Trans.* **1992**, *88* (2), 243–249.
(13) Davis, K. J.; Dove, P. M.; De Yoreo, J. J. *Science* **2000**, *290* (5494), 1134–1137.
(14) Setoguchi, H.; Okazaki, M.; Suga, S. In *Origin, evolution, and modern aspects of biomineralization in plants and animals*; Crick, R. E., Ed.; Plenum Press: New York, 1989; pp 409−418.
(15) Arnott, H. J. In *The mechanisms of biomineralization in animals and plants*; Omori, M., Watabe, N., Eds.; Tokai University Press: Tokyo, 1980; pp 211−218.
(16) Levi-Kalisman, Y.; Raz, S.; Weiner, S.; Addadi, L.; Sagi, I. *Adv. Funct. Mater.* **2002**, *12*, 43–48.
(17) Taylor, M.; Simkiss, K.; Greaves, G.; Okazaki, M.; Mann, S. *Proc. R. Soc. London, Ser. B* **1993**, *252*, 75–80.
(18) Arnott, H. J.; Pautard, F. G. E. In *Biological calcification: cellular and molecular aspects*; Schraer, H., Ed.; Appelton Century Crofts: New York, 1970; 375−446.
(19) Al-Sawalmih, A.; Li, C. H.; Siegel, S.; Fratzl, P.; Paris, O. *Adv. Mater.* **2009**, *21* (40), 4011–4015.
(20) Koga, N.; Nakagoe, Y. Z.; Tanaka, H. *Thermochim. Acta* **1998**, *318* (1−2), 239–244.
(21) Politi, Y.; Batchelor, D. R.; Zaslansky, P.; Chmelka, B. F.; Weaver, J. C.; Sagi, I.; Weiner, S.; Addadi, L. *Chem. Mater.* **2010**, *22* (1), 161–166.
(22) Ramirez, A. P. *Nature* **2003**, *421* (6922), 483–483.
(23) Currie, H. A.; Perry, C. C. *Ann. Bot.* **2007**, *100* (7), 1383–1389.
(24) Sangster, A. G.; Hodson, M. J.; Tubb, H. J. In *Studies in Plant Science*; Datnoff, L. E., Snyder, G. H., Korndörfer, G. H., Eds.; Elsevier: Amsterdam, 2001; Vol. 8, pp 85−113.

JA106883C